


RESEARCH

Open Access



Investigating the bacterial consortia properties of electrogenic anodic biofilm in a double-chamber microbial fuel cell: electrochemical, physical, biochemical and molecular characterization

Doaa Khodary Zater¹, Fatma I. Elzamik¹, Howaida M. Abdel Basit¹, Gamal El-Din M. Moustafa¹, Dena Z. Khater² and Kamel M. El-Khatib^{2*} 

Abstract

This work evaluated the electrochemical, physical, biochemical, and molecular characterization of electrogens from a graphite felt anode when zinc oxide on activated carbon (ZnO/AC) was used as a cathodic electrocatalyst in a double-chambered microbial fuel cell (DCMFC). The electrochemical polarization behavior of the DCMFC showed that ZnO/AC had a higher power density (PD_{max}) of 89 mW m^{-2} with a corresponding cell current density (CD) of 248 mA m^{-2} and a voltage output of 395 mV, which was higher than those of the blank electrode used as a benchmark (PD_{max} of 68 mW m^{-2} at a CD of 161 mA m^{-2} and a voltage of 421 mV). Furthermore, scanning electron microscopy and transmission electron microscopy revealed that the morphology and interior properties of the strains varied among the rods (bacilli), spirals (vibrios), and spheres (diplococci, staphylococci and streptococci). In addition, biochemical characterization via the Vitek2 compact system and molecular analysis via 16 S rRNA and 18 S rRNA gene sequencing revealed the occurrence of nine prevalent species that were correlated with *Sphingobacterium spiritivorum*, *Ochrobactrum anthropicus*, *Pseudomonas mendocina*, *Stenotrophomonas maltophilia*, *Leuconostoc mesenteroides*, *Staphylococcus equorum*, *Bacillus subtilis* HQ334981.1, *Kocuria kristinae* KC581674.1 and *Saccharomyces cerevisiae* NR111007.1. Consequently, the present study outlines different characterization strategies for electrogenic microbes that play an important role in the overall performance of DCMFC for scaling up and managing existing environmental pollution for sustainable energy generation.

Keywords Double-chamber MFC, Electricigens, SEM, TEM, Vitek2, 16S rRNA genes

1 Introduction

Organic pollutants, toxic components, and heavy metal effluents can lead to impurities in water [1]. Consequently, sustainable treatment methods are needed for water recovery and reuse [2]. Microbial fuel cells (MFCs) are suitable for transforming waste directly into electricity through the biochemical process of electrogenic microbes [3]. MFCs allow microorganisms to harvest the electric energy from organic matter by converting the

*Correspondence:

Kamel M. El-Khatib
kamelced@hotmail.com

¹ Microbiology Department, Zagazig University, Zagazig 44511, Egypt

² Chemical Engineering & Pilot Plant Department, Engineering Research and Renewable Energy institute, National Research Centre, Dokki, Cairo 12622, Egypt



© The Author(s) 2024. **Open Access** This article is licensed under a Creative Commons Attribution 4.0 International License, which permits use, sharing, adaptation, distribution and reproduction in any medium or format, as long as you give appropriate credit to the original author(s) and the source, provide a link to the Creative Commons licence, and indicate if changes were made. The images or other third party material in this article are included in the article's Creative Commons licence, unless indicated otherwise in a credit line to the material. If material is not included in the article's Creative Commons licence and your intended use is not permitted by statutory regulation or exceeds the permitted use, you will need to obtain permission directly from the copyright holder. To view a copy of this licence, visit <http://creativecommons.org/licenses/by/4.0/>.

chemical energy stored in pollutants into bioelectricity with high removal rates [4]. The electrons released from the oxidation process are transported into the anode via conductive protein complexes and nanowires [5]. The transfer of electrons between the anode and microbes occurs either by extracellular transfer [6] or by intuitively or synthetically formed redox shuttles [7]. A combination of electrochemical, phylogenetic, and genomic techniques offers opportunities in determining the composition of electroactive species, a better understanding of the extracellular electron transfer process, which in turn can lead to optimization for power output [8].

Thus, necessary techniques are needed to give researchers a view of the appropriate methods. Therefore, physical techniques such as images from scanning electron microscopy (SEM) and transmission electron microscopy (TEM) suggest the chance to recognize and understand the morphology and interior properties of the electrogenic microbes that were previously too hard to be gained by regular techniques. They can introduce evidence that the direct electron transfer (DET) out electrogenic cells into insoluble solid phases by highly conductive nanowires or via membrane-bound c-type cytochrome [9]. Furthermore, biochemical analyses offer the difference between Gram-negative and Gram-positive bacteria, electrogenic and performance activity, and electron transfer via endogenous redox-active metabolites. Also, genomic techniques such as 16 S rRNA provided important information on the structure, metabolic pathway, and genetic potential of colonized biofilm. Moreover, population dynamics is an important indicator of electrochemical activity and biochemical processes [10].

The power generation of an applied MFC is related to several factors, such as the reactor configuration, electrogenic microbes, electrode material, electron donors, separator (such as proton exchange membrane, PEM), and electron acceptors. A typical MFC consists of anodic and cathodic chambers. Classically, the anode section is preserved underneath an anaerobic environment to reduce the influence of oxygen damage on the electrogens and decrease the columbic efficiency. Nevertheless, single-chamber MFCs have a simple and low-cost setup, they have numerous boundaries due to the absence of a membrane in their configuration, including substrate depletion at the cathode and oxygen diffusion to the anode surface, resulting in the competition of O_2 with the anodic electrogenic microbes to accept the produced electrons from the oxidation of the organic substrate, resulting in lowering of bioelectrocatalytic activity of electrogenic, electron recovery, and columbic efficiency [11, 12]. In this regard, dual-chamber MFC configurations have the prospective to overwhelm these

boundaries, according to the existence of an ion-selective separator.

There are numerous compensatory effects of electricigens, such as high efficiency, long stability, and DET. They have been found in a variety of different and complex habitats, including municipal wastewater, salt water, soils and sediments. For example, *Shewanella putrificans* [13], *Geobacter metallireducens* [14], *Geobacteraceae sulfurreducens* [15] and *Rhodospirillum rubrum* [16]. Electrogenic microbes, as pure mixtures of indigenous and engineered artificial bacteria, have been used as anode bioelectrocatalysts [17]. The electron donors used for fuel vary from simple organic substrates such as acetate or complex organic pollutants such as wastewater [18].

Economically, MFCs have not yet been established due to the decreased power yields. The power yields are approximately 54 mW m^{-3} for urban wastewater [19] and range from 250 to 500 mW m^{-2} for wastewater [20]. To optimize the performance of MFCs, electrode materials must be relatively inexpensive, highly conductive, and have a large surface area [21]. Modification of transition metal oxides (e.g., SnO_2 , Cu_2O , ZnO , TiO_2 , CeO_2 , and CO) has attracted significant attention owing to its ability to reduce electrons on cathodic surfaces.

Based on the above description, the foremost objective of the present study was to determine the selection of microbes from a mixed culture that can grow on the anodic carbon felt surface to generate electricity in a double chambered microbial fuel cell (DCMFC) by using zinc oxide supported on activated carbon (ZnO/AC) as a cathodic electrocatalyst. Furthermore, the electricigens were characterized electrochemically by studying the polarization behavior of DCMFCs, and physically by using SEM and TEM. Finally, the electricigen community structures were further identified biochemically by the Vitek2 compact system and molecularly using 16 S rRNA and 18 S rRNA gene nucleotide sequencing analysis. This paper evaluates the use of different characterization approaches for electricigen microbes as biocatalysts for assessing the development of DCMFCs on a large scale for sustainable energy generation.

2 Materials and methods

2.1 DCMFC configuration

Two DCMFCs were assembled by connecting two cylindrical chambers cathodic and anodic chambers. All the bioreactors had a PEM with a diameter of 6 cm between the cathodes and anodes. The carbon felt anodes were three-dimensional (Fuel Cell Store, TX, USA) with an estimated active surface area of approximately 19.5 cm^2 . The cathodes were made of a non-wet proof carbon cloth with a microporous layer (active surface area equal to

16.6 cm²). The electrodes of the bioreactors were connected with stainless steel wires for electron transfer.

2.2 Preparation of the cathodic electrode

ZnO/AC with a mass loading of 0.3 mg cm⁻² was prepared as previously described [22]. First, the ZnO/AC powder was mixed well with a 5% Nafion solution. Then, the resultant mixture was sonicated at 60 °C for 30 min. Afterward, the paste was uniformly distributed on the surface of the carbon cloth electrode. Finally, the cathodic electrode was allowed to dry at room temperature for 24 h before starting the MFC studies. Blank carbon cloth without any modification was used in another DCMFC as a benchmark for comparison.

2.3 Setup and operation

Anodic chambers were injected with aerobic-activated sludge collected from a home-grown wastewater treatment plant (Minia El-Kamh, Sharqia, Egypt). The plants were inoculated with synthetic sodium acetate (2.0 g L⁻¹) as fuel in 50 mM phosphate buffer and minerals (12.5 mL). The buffer solution contained MgCl₂, 3.15; yeast extract, 1.0; NaCl, 0.3; CaCl₂, 0.15; KH₂PO₄, 0.42; NH₄Cl, 0.2; NaHCO₃, 2.5; K₂HPO₄, 1.26; and KCl, 0.33 g L⁻¹ at a COD inlet of 1284 mg L⁻¹. All MFCs were operated in batch-fed mode at a pH of 7 and at room temperature to permit biofilm growth. The cathodic chambers were loaded with 2.0 g L⁻¹ potassium permanganate (KMnO₄) as a catholyte in a cathodic chamber that acted as an electron acceptor at pH=8.3.

2.4 Measurements and calculations

2.4.1 Electrochemical analysis

DCMFCs functioned primarily at an open-circuit cell voltage for three cycles. Subsequently, the system was closed by a 10 kΩ resistor to achieve a steady voltage, sustainable performance of anodic electrogenic microbes in a long-term operation and to select Proteobacteria phylum that can perform anode respiration for electricity generation [23, 24]. A data acquisition system (USB 6000 12 - BIT 10 KS/S Multifunction I/O as well as NI - DAQMX Software) connected to a personal computer for measuring the produced voltage every 5 min. Afterthought, the power and polarization curves were obtained by fluctuating the external loads from 470 kΩ to 240 Ω.

2.4.2 Performance of DCMF analyses

The chemical oxygen demand removal efficiency (COD removal (%)) was calculated as

$$COD_{removal}(\%) = \frac{(COD_{initial} - COD_{final})}{COD_{initial}} \times 100 \quad (1)$$

where COD_{initial} and COD_{final} are the influent and effluent concentrations (mg L⁻¹), respectively, at the end of the DCMFC batch cycles [25].

The coulombic efficiency (C_E) expresses the charge efficiency in which electrons are being transferred in the DCMFC. It was determined by integrating the generated current with the theoretical current as follows:

$$C_E = \frac{CP}{CT} \times 100 \quad (2)$$

where CP is the Coulombs equivalent to the actual current produced during one batch cycle (Coulomb, C). CT is the theoretical coulombs (Coulomb, C) and is estimated according to the following formula: CT = (F × N × W × V)/M, where F is Faraday's constant (96,485 C mol⁻¹), N is number of moles of electrons (8 mol mol⁻¹), W is the daily COD load removed (g L⁻¹), M is the molecular weight of acetate (59 g mol⁻¹), and V is the medium volume (100 mL) [26].

2.4.3 Physical analyses of biofilms

The interior morphology of the isolated strains was studied using field emission scanning electron microscopy (FESEM) and high-resolution TEM (HRTEM). Therefore, the formed anodic biofilm was removed and envisioned after batch cycles to confirm the role of the anodic biofilm in electricity liberation using previously described standard processes [27].

2.4.4 Biochemical and molecular analyses of isolated strains

The isolated biomass on anodic carbon felt was harvested at the end of the batch cycles of DCMFC. Then, the cells were placed in a flask containing 90 mL of phosphate buffer solution. After that, the flask was stirred for 2 h, and the solutions were diluted to 1 × 10⁻⁷. The facultative anaerobic bacteria were isolated using sterile sodium thioglycollate agar (1.5 KH₂PO₄, 0.5 cysteine HCl, 5.0 yeast extract, 15.0 peptone, 3.0 sodium acetate, 5.5 glucose, 0.001 sodium resazurin, 20 agar, 0.5 sodium thioglycollate, 2.5 NaCl, and 2.0 K₂HPO₄ g L⁻¹). For 3 d, the plates were incubated at 37 ± 2.0 °C for colony-forming units (CFU) in the selected petri dishes. Plate count agar (PCA) medium was used to isolate aerobic bacteria, which were incubated at 28 ± 2.0–48 h. To isolate the yeast strains, media containing 10% glucose, 3% yeast extract, 0.6% NaH₂PO₄, 0.2% NH₄Cl, and 0.05% MnSO₄ g L⁻¹ were used at pH=6.3. For the CFUs, the selected Petri dishes were incubated at 28–30 ± 2.0 °C for 48 h. To confirm their purity, the former colonies were picked and spread onto the same media.

Biochemical characterization by vitek2 Six isolated electricigens were identified by the Biomeriux VITEK 2

compact method [28]. The isolated strains were transported and mixed well by a sterilized swab into a polystyrene test tube containing 3 mL of sterile saline. To adjust the turbidity, a VITEK®2 DensiCHEK™ turbidity meter was used. The microbe biomass was retained in a cassette and subsequently placed into a vacuum chamber station. The obtained data were collected, and a special algorithm was used to exclude incorrect interpretations. Finally, the results were automatically obtained and recorded after 10 h, as previously mentioned [29].

16 S rRNA and 18 S rRNA gene sequencing Three unidentified microbes by the vitek2 compact method were cultured in sterile plant tubes containing specific media (PCA) and incubated before being sent to Macrogen® (Korea) for molecular identification by 16 S rRNA and 18 S rRNA gene sequencing. The DNA of the particular isolates was used as a template for Polymerase Chain Reaction (PCR) with the three primer pairs shown in Table 1. PCR amplification was performed with a Gene Amp 2400 PCR system according to the following program: first, denaturation at 95 °C for 5 min for each denaturation for 1 min; second, annealing at for 1 min; and extension at 72 °C for 2 min. The extension of the primer segment was prolonged at 72 °C for 5 min in the final round. Consequently, the PCR products were resolved via electrophoresis on a 1.2% agarose gel at 80 V for 1 h with 1X Tris base, Acetic acid and EDTA buffer and then stained with ethidium bromide solution for approximately 10–15 min.

The amplified fragments were examined via visualization under a UV trans illuminator. The PCR products were amplified from the DNA extracts of the isolates, purified, and sequenced using the ABI PRISM (BigDye™ Terminator Cycle Sequencing Kit). Single-pass sequencing was performed on each template using identical primer pairs according to the protocol provided by the manufacturer. The samples were resuspended in distilled water and subjected to electrophoresis in a

sequencer (ABI 3730xl). The microbial isolate sequences of DNA (labeled Sh-02, Sh-07 and Sh-05) were subsequently associated with the universal isolate nucleotide sequences collected from <http://www.ncbi.nlm.nih.gov/>, using the DNASTAR Software Package-Laser Gene (Expert Sequence Analysis Software, USA) and the MEGA Align database.

Attachment and biomass assay The previously identified strains were tested for biomass and biofilm formation according to a previously described method [30]. The wells of a sterile 96-well polystyrene microplate (Brand, Wertheim, Germany) were filled with 150 µL aliquots of prepared suspension culture and fresh Luria–Bertani (LB) broth. Then, the plates were incubated at 37 °C for 24 h. Thereafter, using an ELISA reader (Thermo Scientific Multiskan FC, USA) and a computer with evaluation software, the biomass concentration was estimated by optical density measurement at OD₆₀₀ nm. Subsequently, the content of each well was removed by aspiration, and the samples were rinsed three times with 250 µL of sterile distilled water. The attached bacteria were fixed with 200 µL of methanol for 15 min, emptied, and dried at room temperature. Afterward, 200 µL of a 5% (v/v) crystal violet solution (Fluka) was added to each well and held at ambient temperature for 15 min. Later, the plate was placed under gently running tap water to remove the excess stain. To release the stain from adherent cells, 33% (v/v) glacial acetic acid was added. Biofilm formation was measured using an ELISA reader at an OD570.

3 Results and discussion

3.1 Electrochemical characterization

3.1.1 Stability of DCMFCs

DCMFCs were assessed in fed-batch mode to promote the dynamic acclimation of mature electrogenic anodic biofilms using acetate as fuel and ZnO/AC as a cathodic electrocatalyst in comparison to blank cathodic electrodes. Figure 1a shows that the measured open circuit potentials (OCVs) increased over three consecutive

Table 1 The nucleotide sequences of the primer pairs were used for the molecular identification of electricigens

Genes	Primer pairs	Nucleotide sequences (5'.....3')	
16 S rRNA	Pair A	518 F	CCAGCAGCCGCGGTAATACG
		800R	TACCAGGGTATCTAATCC
	Pair B	785 F	GGATTAGATACCCTGGTA
		907R	CCGTCAATTCMTTTRAGTTT
18 S rRNA	Pair C	NS1	GTAGTCATATGCTTGCTC
		NS24	AAACCTTGTTACGACTTTTA

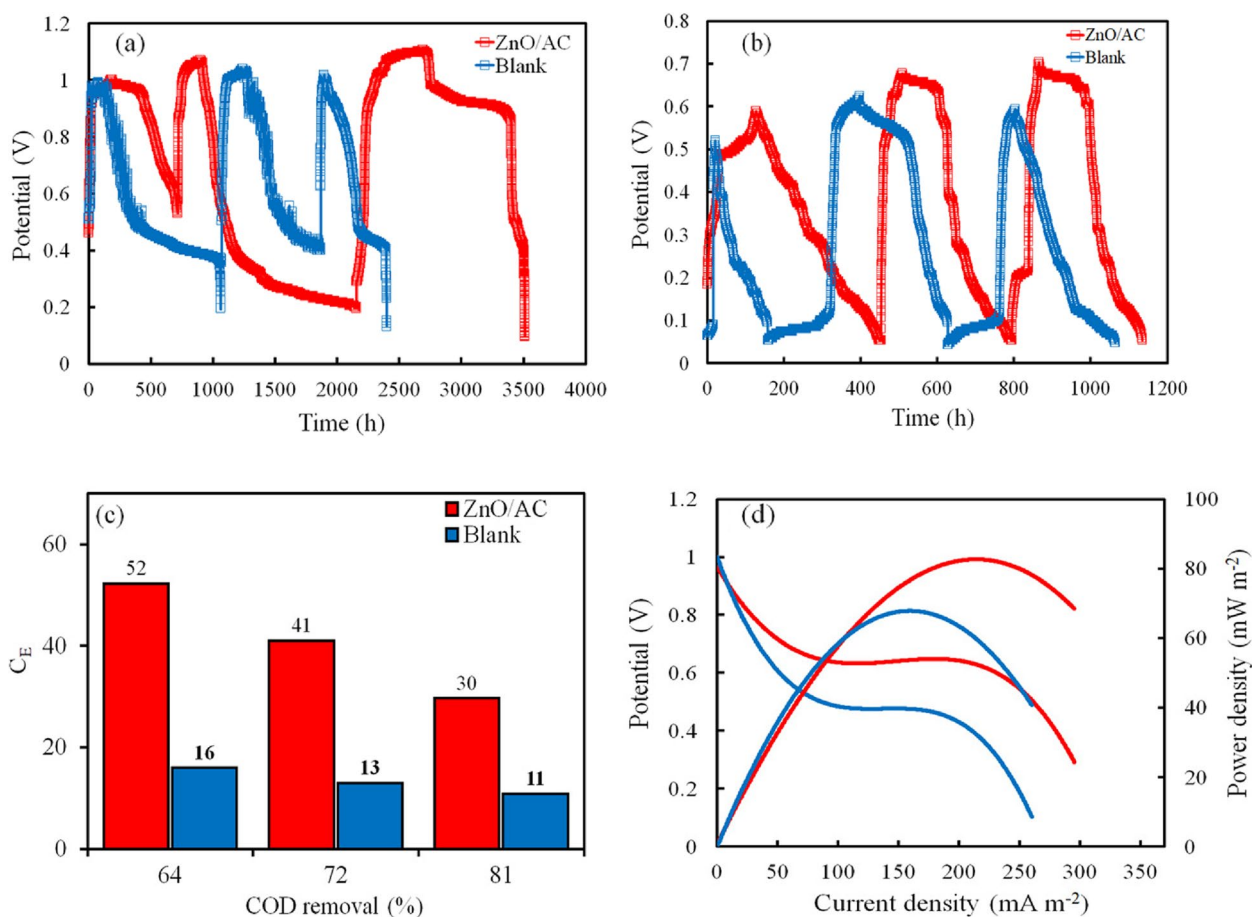


Fig. 1 a OCVs; b CCVs; c C_E vs. COD removal; d Polarization and power outputs of ZnO/AC and blank DCMFCs

cycles in the fed-batch. In the first operating cycle, the OCVs increased successively to values reaching 1.00 and 0.98 V after 7 and 4 d for the ZnO/AC and blank DCMFCs, respectively. Then, the voltage was gradually reduced according to the reduction in microbial cell viability at the end of each cycle for each DCMFC due to the consumption of acetate. Afterward, the anode chambers were inoculated with fresh media introduced after each cycle to revive the anodic electrode with active microorganisms and accelerate anodic biofilm formation each cycle. As a consequence, the OCVs increased again, reaching 1.07 and 1.03 V after 17 and 11 d of operation before the drop phase for the ZnO/AC and blank DCMFCs, respectively. In the third operating cycle, the OCVs attained maximum stable values of 1.11 and 1.04 V after 23 and 7 d for the ZnO/AC and blank DCMFCs, respectively. It could be concluded that the OCV results might be attributed to the successful development of an electrogenic biofilm that improved voltage and electricity generation.

3.1.2 Performance of DCMFCs

Figure 1b depicted the influence of 10 k Ω on the performance of DCMFCs at a preliminary concentration of sodium acetate (2 g L $^{-1}$) in batch mode as an electron donor and KMnO $_4$ as an electron acceptor after 150 d. During three operating cycles, the closed-circuit voltages (CCVs) behaved in the same manner as the OCVs. In addition, the ZnO/AC-based DCMFC had a slightly greater maximum CCV output of 0.65 ± 0.06 V than that of the blank (0.58 ± 0.06 V). Hence, the performance of ZnO/AC-based DCMFCs was correlated with both anodic and cathodic electrocatalyst activities [31]. The percentage of COD removal and C_E during the progression of MFC operation at 10 k Ω and an initial COD of 1284 mg L $^{-1}$ were shown in Fig. 1c. The superior CODs were achieved over three closed cycles by approximately 87, 91 and 94% with decreasing COD concentration in the ZnO/AC-based DCMFC when compared to that of the blank cathode at 65, 72 and 81%, respectively. As a result, the ZnO/AC-based DCMFC behavior was correlated

with acetate breakdown by electricigens and an increased reduction rate in the cathodic chamber using the electroactive catalyst ZnO/AC, resulting in a lower COD value. Moreover, the C_{Es} over three cycles were greater for ZnO/AC (52, 41, and 30) than for the blank (16, 13 and 11). Consequently, an inverse relationship between C_E and substrate concentration was established.

3.1.3 Polarization and power outputs

The illustrative corresponding power density and steady-state polarization characteristic plots for ZnO/AC and blank DCMFC were elaborated by applying different external resistances fluctuating from 470 k Ω to 240 Ω in reducing order stepwise after the MFC was operated stably. As shown in Fig. 1d, when the current density was 248 mA m⁻² and the consistent voltage output was 395 mV, the PD_{max} was 89 mW m⁻² for ZnO/AC. On the other hand, the blank cathode generated a high power density of 68 mW m⁻² at a cell current density of 161 mA m⁻² and a corresponding voltage output of 421 mV. Furthermore, the internal resistance (R_{in}) was calculated and was approximately lower for ZnO/AC (1.3 k Ω) than for the blank (1.5 k Ω). This difference might be due to the electron-transfer kinetics of the oxygen reduction on the ZnO/AC cathode.

As illustrated in Table 2, these results exhibited greater power output performance than those done by Mathew and Thomas, in which a lower power density (7 mW m⁻²) was obtained from the DCMFC when PANI-ZnO was loaded on stainless steel mesh. However, using PANI-Cu/ZnO, a PD of 45 mW m⁻² was achieved [32]. Moreover, Tajdid Khajeh et al. evaluated CuO/ZnO-modified graphite plates in a DCMFC and reported a PD of 51 mW m⁻² under visible light irradiation [33]. In addition, the performance was lower than that of a previous study, which was performed by Dessie et al. They produced a PD of 506 mW m⁻² when

using α -MnO₂/NiO/PANI as a cathodic electrocatalyst and *Escherichia coli* as an electroactive microorganism anodic electrocatalyst in DCMFCs [34]. This variation in power density might be related to many variables, including the operating environment, MFC structure, anode type, surface area, microbial community variations, electron acceptors, PEM, changes in catalyst-supporting components and their anticipated surface area.

3.2 Physical characterization of electroactive isolated biofilms

3.2.1 SEM analysis

From previous electrochemical studies, it could be assured that the mature electroactive anodic biofilm could oxidize acetate and liberate the produced electrons into the anodic electrode. After that, as illustrated in Fig. 2a, these liberated electrons were transferred into the cathode through an external resistor of 10 k Ω to generate electricity through the reduction of potassium permanganate as a catholyte in the presence of ZnO/AC as an electrocatalyst on the cathodic side. Hence, the physical characteristics of the isolated biofilm that was responsible for bioelectricity generation were visualized at the end of the operation (7 months) via SEM analysis.

This analysis was used to examine the morphologies of the plain carbon felt and the anodic biofilm that accumulated on the carbon-felt electrodes. As illustrated in Fig. 2b, the superficial morphology of the plain carbon felt was highly flat, with numerous carbon fibers overlapping one another to form a mesh-like structure. On the other hand, the morphological structure, cell attachment, topography, and distribution of the bacterial biofilm on the anodic carbon-felt surface are shown in Fig. 2c. The images showed the presence of rod, coccid, and clustered-shaped cells closely linked with the graphitic

Table 2 Comparison of the current study with the literature

Cathode catalyst	Substrate	Culture	MFC configuration	OCV (V)	CCV (V)	COD %	C_E	Power density mW m ⁻²	Ref.
ZnO/AC	Acetate	Activated sludge	DC	1.11	0.65	94	52	89	This study
ZnO/AC	Acetate	Activated sludge	SC	0.56	0.30	76	9	90 mW m ⁻³	[22]
PANI-Cu/ZnO	Wastewater	Food wastewater	DC	0.09	-	-	-	45	[32]
CuO/ZnO	Milk AO7	Anaerobic sludge	DC	0.36	-	82	1	51	[33]
α -MnO ₂ /NiO/PANI	Glucose	<i>E. coli</i>	DC	0.71	-	82	10	506	[34]
PPY/CNT/CP	Palm oil	Anaerobic sludge	DC	0.26	0.22	96	21	113	[35]
0.3%CNT/Pt/CP	Palm oil	Anaerobic sludge	DC	0.79	0.44	88	47	143	[36]
ZnO NPs/Co	Acetic acid	Potato wastewater	SC	1.58	0.25	80	-	0.37	[37]
Cel-PDA/TiO: ZnO	Acetate	Textile wastewater	SC	1	0.74	60	-	63	[38]

DC double chamber, SC single chamber, OCV open circuit potential, CCV close circuit potential, COD removal efficiency, C_E coulombic efficiency

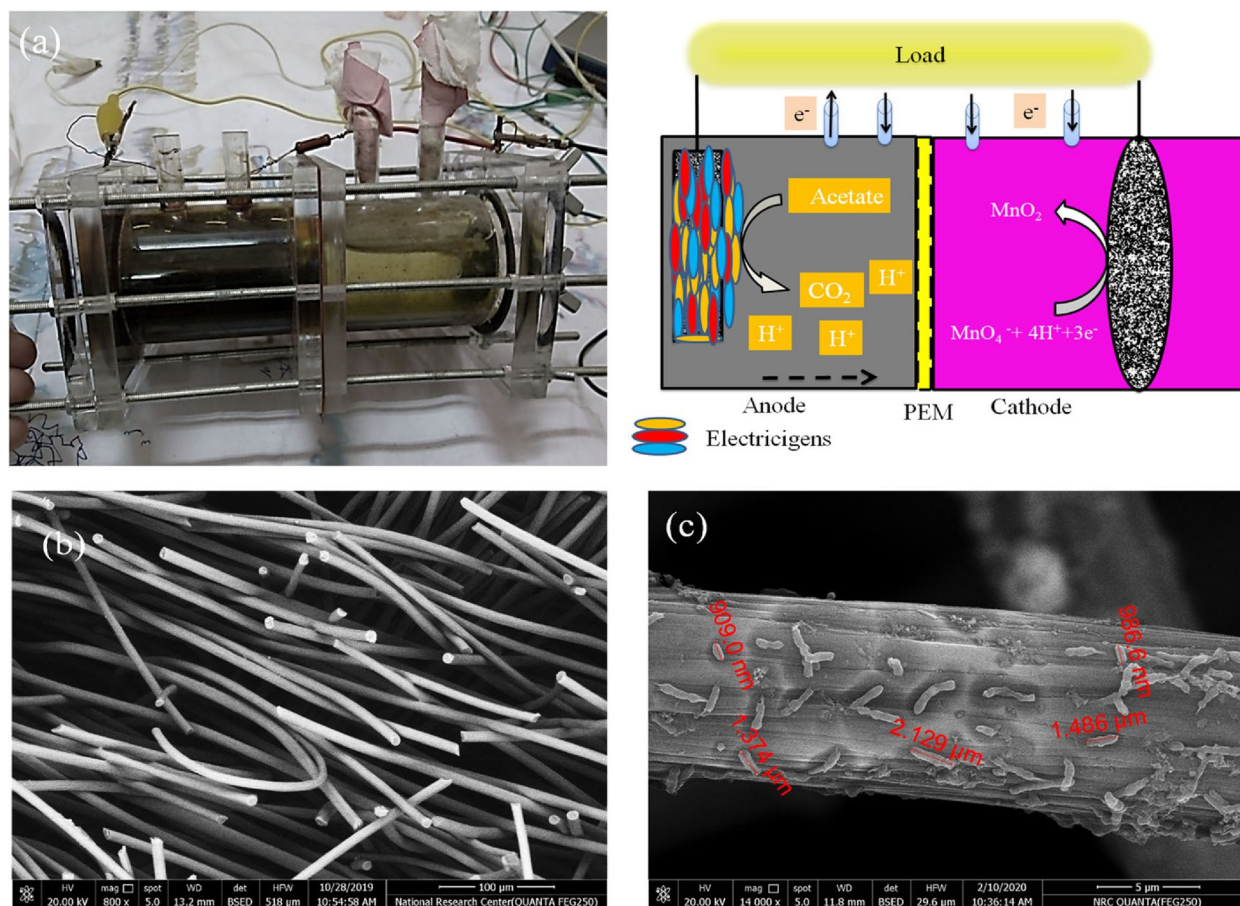


Fig. 2 a DCMFC photograph with schematic details; b and c SEM of anode before and after inoculation

surface, approximately 0.9 to 2.1 μm long, which produced electricity owing to the presence of electrogenic biofilms. Furthermore, the anodic carbon felt was supposed to signify an appropriate place for the anaerobic augmentation of anodic biofilms.

3.2.2 TEM analysis

The interior structure and microbial physiology of the isolated electricigen communities from the surface of the anodic electrode that was responsible for bioelectricity generation were examined via TEM. The TEM images of isolates (donated as a to j) were illustrated in Fig. 3, which demonstrates how the ultrastructure of each isolate differed from that of the rod (bacilli) surface, as indicated in (Fig. 3a - e); spiral (vibrio) surface (Fig. 3f and g); and sphere surface that could be encapsulated by diplococci, staphylococci and streptococci (Fig. 3h and j). Furthermore, as shown in (Fig. 3f and g), there was a filamentous structure on the surface of spirals known as a nanowire (pili). Major cellular ultrastructural characteristics were also discovered in lipid membranes and the cytoplasm.

The lateral dimension thickness of the layers ranged from 200 nm to 1 μm .

Based on the TEM analysis results of the present study, it could be assumed that the transfer of electrons from the respiratory chain of the microbe cell to an external electron acceptor surface (anode) was catalyzed by two direct major pathways, as illustrated in Fig. 4. The first pathway is DET, which occurs through physical interaction between a microbe's cell and anode without the contribution of any redox species [39]. An additional form of DET is the conductive pili (nanowire). The second pathway involves mediated electron transfer (MET), which occurs via redox shuttles [40].

3.3 Biochemical identification using the vitek2 compact system method

The biochemical analysis using the Vitek2 compact system revealed the presence of six discrete foremost bacterial species that were classified as Gram-negative (four) or Gram-positive (two) as demonstrated in Table 3. The Gram-negative species were *Sphingobacterium*

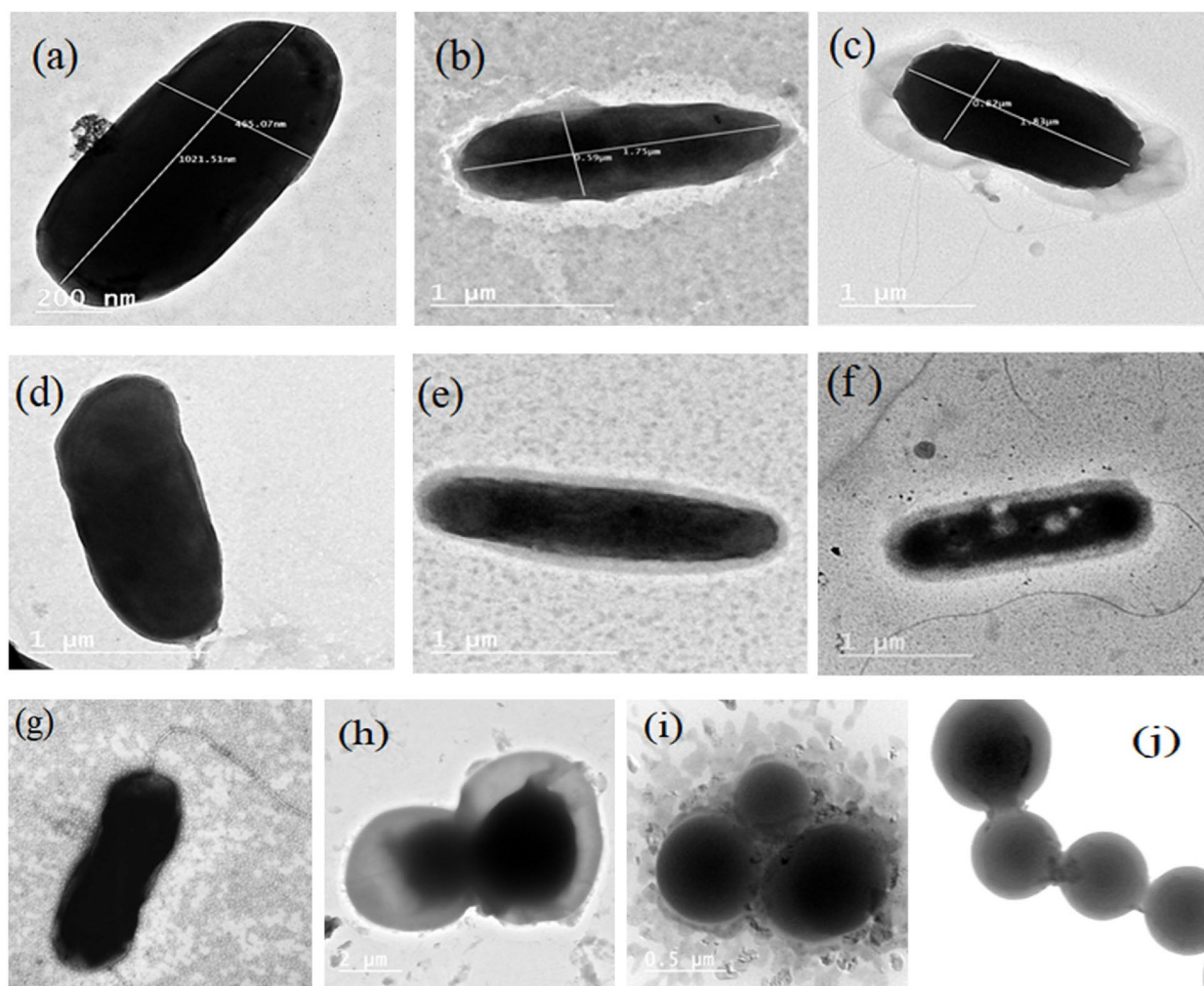


Fig. 3 TEM images of isolated electricigens from anodic biofilm

spiritivorum, *Ochrobactrum anthropicus*, *Pseudomonas mendocina*, and *Stenotrophomonas maltophilia*. On the other hand, *Leuconostoc mesenteroides* and *Staphylococcus equorum* were Gram-positive species.

The *S. maltophilia* and *O. thraipi* species are facultatively anaerobic, motile by polar flagella and able to produce electricity through their flagellum (nanowire) [41]. Previous research on the microbial electrochemical remediation of hydrocarbons revealed the prevalence of *Stenotrophomonas* spp. and their dominance in anodic microbial populations [42]. *S. spiritivorum* and *P. mendocina* are facultative anaerobic, nonfermentative, nonmotile, nonspore-forming bacilli. These species were previously identified in anodic biofilm electrodes in MFCs [43]. *L. mesenteroides* and *S. equorum* are facultatively anaerobic, streptococcal and grape-like cluster shapes, respectively. Previously, Flimban et al. reported that six species of *Staphylococcus* isolated from MFCs

might be important in future biofuel research [44]. However, there are no reports on the use of *L. mesenteroides* in MFCs. Additional research will be required to determine the role of this microorganism in determining its electrogenicity in the application of MFCs. Therefore, it could be concluded that biochemical analysis of anodic bacterial populations potential strategy for isolating electrochemically active bacterial microorganisms from activated sludge.

3.4 Molecular analysis by 16SrRNA

Three unidentified electricigen species by the Vitek2 compact system were molecularly identified based on the nucleotide sequences of the 16SrRNA and 18SrRNA genes. This analysis revealed the coexistence of two bacterial strains and one fungal isolate. Figure 5 illustrates the phylogenetic assessment of the unidentified isolated taxa at the genus level. Furthermore, the relative

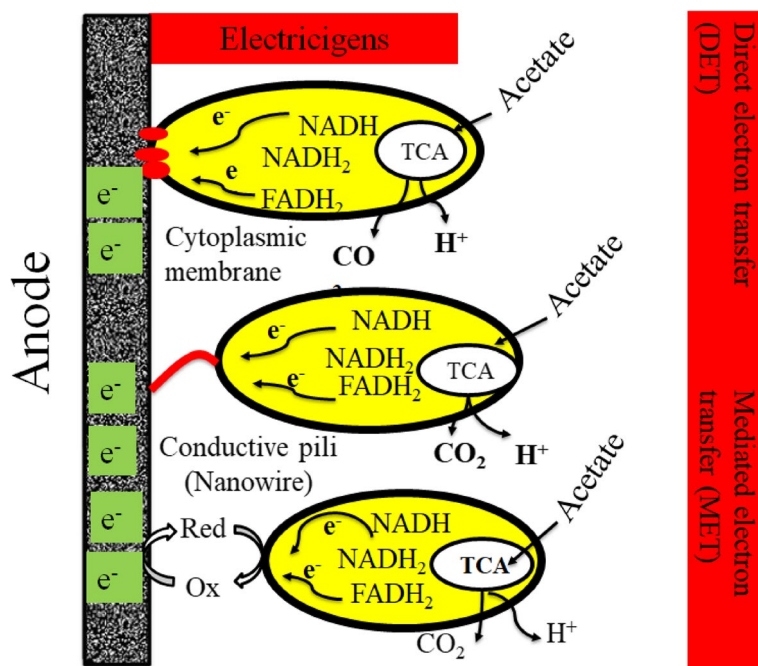


Fig. 4 DET and MET pathways identified in the present study via TEM analysis

proportions of three dominant electricigens that were associated with *Bacillus subtilis* HQ334981.1, *Kocuria kristinae* KC581674.1, and *Saccharomyces cerevisiae* NR111007.1 were determined. Based on the NCIB taxonomic database, the dynamics of the greatest relative abundances (%) of these microbial communities among phylogenetically related species were illustrated in Table 4. The highest relative abundances of *B. subtilis* HQ334981.1, *K. kristinae* KC581674.1, and *S. cerevisiae* NR111007.1 were 99%, 94%, and 95% respectively.

Based on both the Vitek2 compact system and molecular analysis of the 16SrRNA genes revealed the most prevalent Proteobacteria, Firmicutes, Bacteroidota, Ascomycota, and Actinobacteria taxa, which was similar to the findings of previous studies [45]. Members of Bacteroidetes and Firmicutes are well known to ferment polysaccharides (which act as fermentors) to provide metabolic constituents for electrogens [46]. However, members of the Proteobacteria phylum can perform anode respiration. Thus, these isolated strains were correlated with the foremost species that were used for bioelectricity production in MFCs. By playing a vigorous character in the oxidation of sodium acetate and transfer of resulted electrons from their cell into the anodic carbon felt without the addition of an external mediator. Subsequently, reducing the internal resistance with increasing voltage output and subsequently achieving the highest power density [47].

3.5 Biomass concentration and biofilm formation

The previously identified strains (9 strains) were tested for biomass and biofilm formation in microtiter plate wells that were filled with 150 μ l aliquots of prepared suspension culture and LB broth. As illustrated in Fig. 6a; Table 5, there was variation in biomass aggregation among all the strains at OD₆₀₀ nm compared with that of the negative control (NC) (0.16). Among the other tested strains, *S. spiritivorum* had the most biomass formation (1.96), followed by *S. cerevisiae* NR111007.1 (1.87), *L. mesenteroides* (1.86) and *B. subtilis* HQ334981.1 (1.84). Furthermore, as shown in Fig. 6b, variation in biofilm formation was measured at OD₅₇₀ nm values ranging from 0.15 to 0.31 for all the strains. *K. Kristinae* KC581674.1 provided the most biofilm formation (0.31), followed by *S. equorum* and *P. mendosina*, which had the same OD value (0.26). These findings demonstrated that the majority of the identified strains were able to form biofilms at a noteworthy level, which highlights the crucial importance of these microorganisms [48]. In addition, biofilm formation begins with the initial attachment of the bacterium to a surface, followed by the formation of micro-colonies, which leads to the maturation of the micro-colonies into three-dimensional structures that are bound and alleviated by further polymeric substances (EPS) [49].

Table 3 Biochemical analysis details of isolated anodic communities

Characteristic	Isolates (Ve ⁻)				Characteristic	Isolates (Ve ⁺)	
	1	2	3	4		5	6
APPA	+	-	+	+	AMY	-	-
H2S	-	-	-	-	APPA	-	-
BGLU	+	-	-	+	LeuA	-	-
ProA	-	+	+	+	AlaA	-	-
SAC	+	-	-	-	dRIB	-	+
ILATK	-	+	+	+	NOVO	-	+
GlyA	-	+	-	-	dRAF	-	-
O129R	-	-	+	-	OPTO	-	+
ADO	-	-	-	-	PIPLC	-	-
BNAG	-	-	-	+	CDEX	-	-
dMAL	-	-	-	-	ProA	-	-
LiP	+	-	+	+	TyrA	-	-
dTAG	+	+	-	-	ILATK	-	+
AGLU	-	-	(+)	-	NC65	+	+
ODC	-	-	-	-	O129R	-	+
GGAA	-	-	-	+	dXYL	-	+
PyrA	-	+	-	-	AspA	-	-
AGL TP	+	-	-	+	BGURr	-	+
dMAN	+	-	-	-	dSOR	-	+
PLE	-	-	-	-	LAC	+	+
dTRE	+	-	-	-	dMAN	-	+
SUCT	-	+	+	-	SAL	-	-
LDC	-	-	-	-	ADH1	-	+
IML Ta	-	-	+	-	BGAR	-	-
IARL	-	-	-	-	AGAL	-	-
dGLU	+	-	+	-	URE	+	+
dMNE	+	-	-	-	NAG	-	-
TYrA	+	+	+	+	dMNE	-	+
CIT	-	-	+	-	SAC	-	+
NAGA	-	-	-	-	BGAL	(+)	+
IHISa	-	-	+	-	AMAN	-	-
ELLM	-	+	-	-	PyrA	-	+
dCEL	+	-	-	-	POL YB	-	-
GGT	-	-	-	+	dMAL	-	+
BXYL	+	-	-	-	MBdG	-	-
URE	-	+	-	-	dTRE	-	+
MNT	-	-	+	+	AGLU	-	-
AGAL	-	-	-	-	PHOS	-	-
CMT	-	-	-	-	BGUR	-	+
ILATa	-	-	+	-	dGAL	-	+
BGAL	+	-	-	-	BACI	-	+
OFF	-	-	-	-	PUL	-	-
BALaP	-	+	-	-	ADH2s	-	-
dSOR	-	-	-	-			
5KG	-	-	-	-			
PHOS	-	-	-	+			
BGUR	-	-	-	-			
Probable identity	<i>S. spiritivorum</i>	<i>O. anthropic</i>	<i>P. mendocina</i>	<i>S. maltophilia</i>		<i>L. mesenteroides</i>	<i>S. equorum</i>

+ positive, - negative, v variable

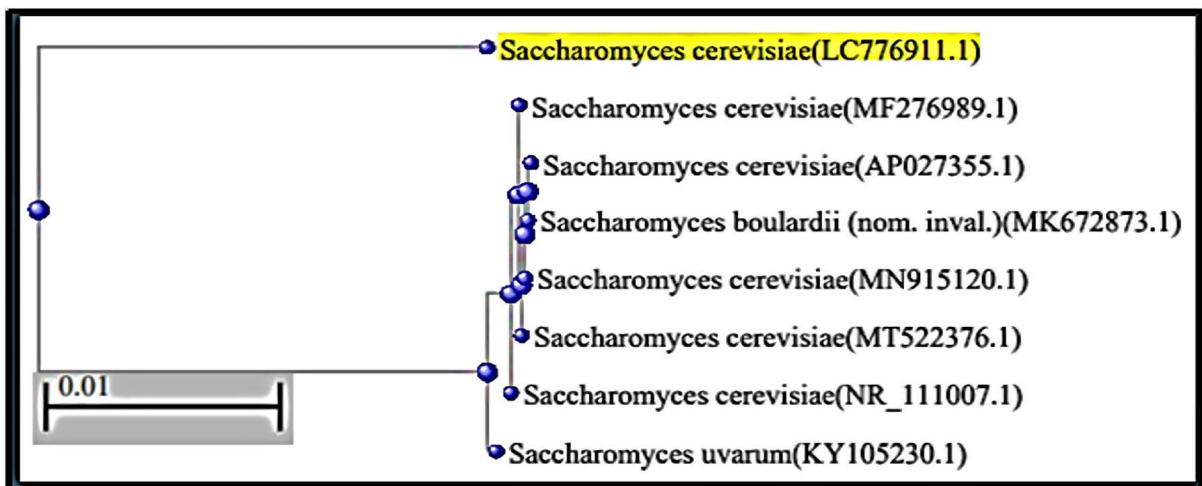
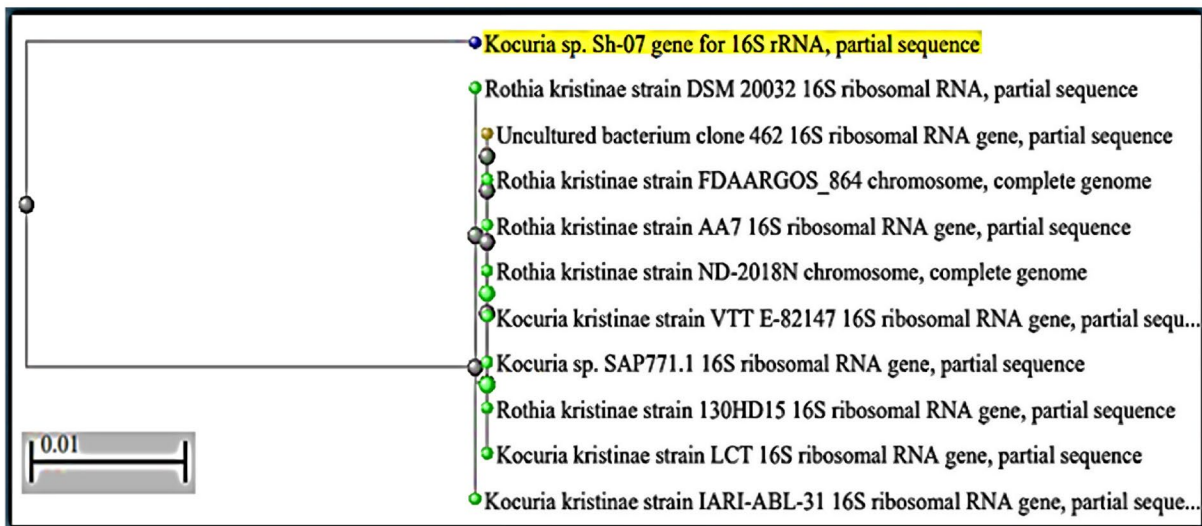
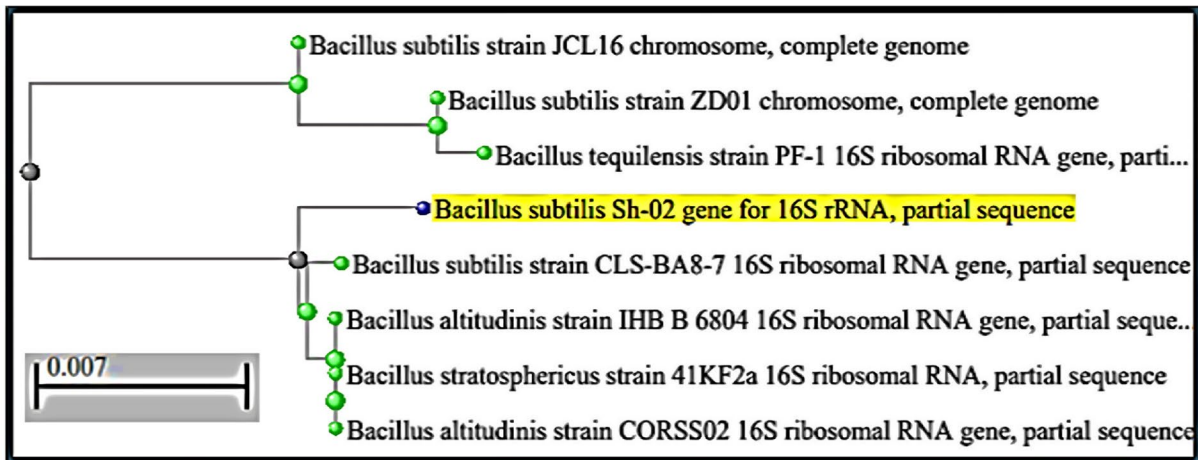


Fig. 5 Phylogenetic relationships of the identified electrogenic species according to the GenBank

Table 4 Sequences producing significant alignments of the 16 S rRNA gene of isolates compared to the most similar strains documented in the GenBank of NCBI database

Description	Query Cover (%)	Identities (%)	Accession
<i>Bacillus subtilis</i> strain CLS-BA8-7 16 S ribosomal RNA gene, partial sequence	100	99	HQ334981.1
<i>Bacillus stratosphericus</i> strain 41KF2a 16 S ribosomal RNA, partial sequence	97	99	NR042336.1
<i>Bacillus altitudinis</i> strain IHB B 6804 16 S ribosomal RNA gene, partial sequence	97	99	KF668457.1
<i>Bacillus altitudinis</i> strain CORSS02 16 S ribosomal RNA gene, partial sequence	97	99	MF425586.1
<i>Bacillus subtilis</i> strain ZD01 chromosome, complete genome	97	96	CP046448.1
<i>Bacillus subtilis</i> strain JCL16 chromosome, complete genome	97	96	CP054177.1
<i>Bacillus tequilensis</i> strain PF-1 16 S ribosomal RNA gene, partial sequence	97	96	OM943768.1
<i>Kocuria kristinae</i> strain IARI-ABL-31 16 S ribosomal RNA gene, partial sequence	100	94	KC581674.1
<i>Rothia kristinae</i> strain DSM 20,032 16 S ribosomal RNA, partial sequence	100	94	NR026199.1
<i>Rothia kristinae</i> strain AA7 16 S ribosomal RNA gene, partial sequence	100	93	MT275600.1
<i>Kocuria kristinae</i> strain VTT E-82,147 16 S ribosomal RNA gene, partial sequence	100	93	KU321256.1
<i>Rothia kristinae</i> strain ND-2018 N chromosome, complete genome	100	93	CP113782.1
<i>Kocuriakristinae</i> strain LCT 16 S ribosomal RNA gene, partial sequence	100	93	KR230389.1
<i>Rothia kristinae</i> strain 130HD15 16 S ribosomal RNA gene, partial sequence	100	93	MW820221.1
<i>Kocuria</i> sp. SAP771.1 16 S ribosomal RNA gene, partial sequence	100	93	JX067686.1
<i>Rothia kristinae</i> strain FDAARGOS_864 chromosome, complete genome	100	93	CP065738.1
Uncultured bacterium clone 462 16 S ribosomal RNA gene, partial sequence	100	93	DQ158132.1
<i>Saccharomyces cerevisiae</i> CBS 1171 ITS region; from TYPE material	99	95	NR111007.1
<i>Saccharomyces cerevisiae</i> isolate 10-1356 internal transcribed spacer 1, and large subunit ribosomal RNA gene, partial sequence	99	95	MF276989.1
<i>Saccharomyces cerevisiae</i> YKN1419 DNA, chromosome 12, nearly complete sequence	99	95	AP027355.1
<i>Saccharomyces uvarum</i> culture CBS:2444 small subunit ribosomal RNA gene, and large subunit ribosomal RNA gene, partial sequence	99	95	KY105230.1
<i>Saccharomyces boulardii</i> (nom. inval.) isolate 10-TS4_reverse internal transcribed spacer 1, and large subunit ribosomal RNA gene, partial sequence	99	95	MK672873.1
<i>Saccharomyces cerevisiae</i> isolate CuricoValley_5 internal transcribed spacer 1, and 5.8 S ribosomal RNA gene, complete sequence	99	95	MN915120.1
<i>Saccharomyces cerevisiae</i> strain T15-20 internal transcribed spacer 1, partial sequence and 5.8 S ribosomal RNA gene, complete sequence	99	95	MT522376.1

4 Conclusions

This study documented a combination of different characterization approaches for electricigens that were isolated from anodic biofilms when ZnO/AC was used as a cathode electrocatalyst in DCMFC operation as electrochemical, physical, and genomic techniques that offer opportunities in determining the composition of electroactive species, better understanding of the extracellular electron transfer process, which in turn can lead to optimization for power output to give researchers a view of the appropriate methods. Electrochemically, ZnO/AC exhibited a higher power density (PD_{max}) of 89 mWm^{-2} with a corresponding cell CD of 248 mA m^{-2} and a voltage output of 359 mV, which were greater than those of the CC electrode (PD_{max} of 68 mW m^{-2} at a CD of 161 mA m^{-2} and a voltage of 421 mV). Furthermore, SEM and TEM showed that all the ultrastructures of the

rods (bacilli), spirals (vibrios), and spheres (diplococci, staphylococci, and streptococci) varied. These analyses can introduce evidence that the direct electron transfer out of electrogen cells into insoluble solid phases by highly conductive nanowires or via membrane-bound c-type cytochrome. Both the Vitek2 compact system and molecular analysis of the 16SrRNA and 18SrRNA genes offer the difference between Gram-negative and Gram-positive bacteria, electrogenic and performance activity, electron transfer via endogenous redox-active metabolites, metabolic pathway, and genetic potential of colonized biofilm. In addition, they revealed the relative proportions of nine dominant electricigen species related to *Sphingobacterium spiritivorum*, *Ochrobactrum anthropic*, *Pseudomonas mendocina*, *Stenotrophomonas maltophilia*, *Leuconostoc mesenteroides*, *Staphylococcus equorum*, *Bacillus subtilis* HQ334981.1, *Kocuria kristinae*

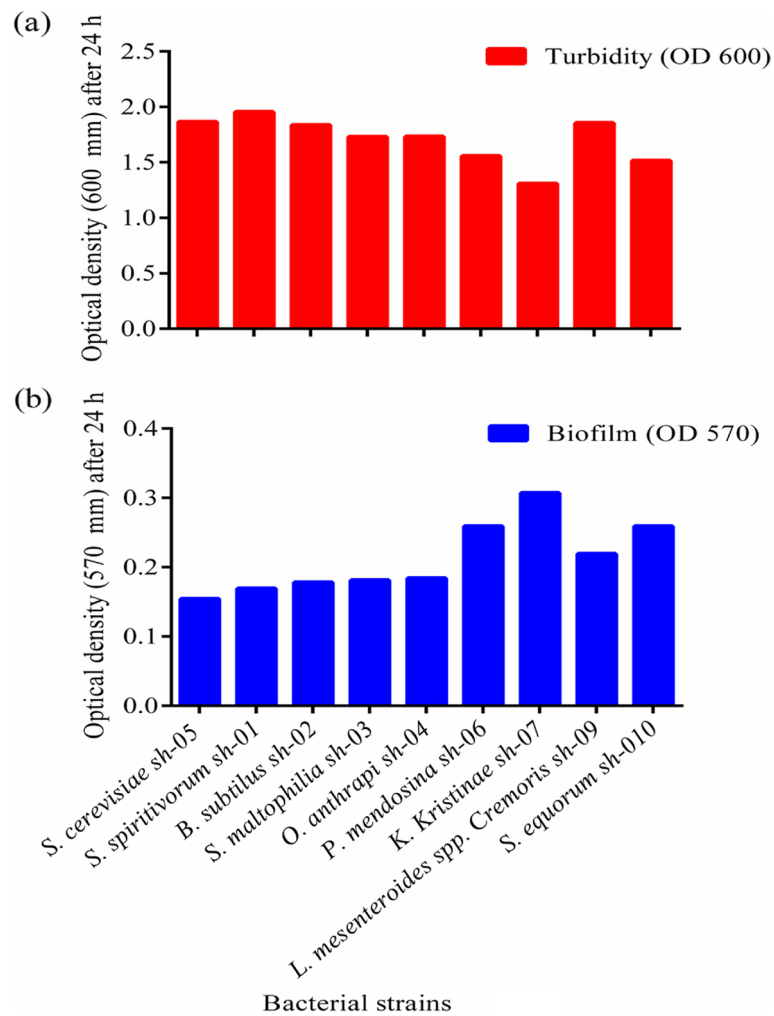


Fig. 6 a Biomass assay and b biofilm formation for the nine identified strains

Table 5 Biomass and biofilm assay for nine different strains at OD₅₇₀ and OD₆₀₀, respectively

NO.	Strains	Biofilm (OD ₅₇₀)	Turbidity (OD ₆₀₀)
1	<i>S. cerevisiae</i> sh-05 AN: LC776911.0	0.15 ^h	1.87 ^b
2	<i>S. spiritivorum</i> sh-01	0.17 ^g	1.96 ^a
3	<i>B. subtilis</i> sh-02 AN: LC776908.1	0.18 ^f	1.84 ^d
4	<i>S. maltophilia</i> sh-03	0.18 ^e	1.73 ^e
5	<i>O. anthrapi</i> sh-04	0.18 ^d	1.73 ^f
6	<i>P. mendosina</i> sh-06	0.26 ^b	1.56 ^g
7	<i>K. Kristinae</i> sh-07 AN: LC776909.1	0.31 ^a	1.31 ⁱ
8	<i>L. mesenteroides</i> spp. <i>Cremoris</i> sh-09	0.22 ^c	1.86 ^c
9	<i>S. equorum</i> sh-010	0.26 ^b	1.52 ^h
	NC*	0.10	0.16

NC* = negative control (medium only). Different letters represent significant differences (Duncan's test indicates a significant difference at $p < 0.05$) among all treatments

KC581674.1 and *Saccharomyces cerevisiae* NR111007.1. These previous strains were correlated with the most dominant phyla, Proteobacteria, Firmicutes,

Bacteroidetes, Ascomycota and Actinobacteria, which were used for bioelectricity generation. According to the findings of the present study, additional attention will be

required toward the mechanism of the liberation of electrons from electricigens cells toward the anode electrode and the development of DCMFCs for commercialization and pilot-scale application in sustainable energy generation and environmental pollution control.

Acknowledgements

We would like to acknowledge the financial support from the Microbiology Department, Faculty of Agriculture, Zagazig University, Egypt. Furthermore, we would like to thank the National Research Centre for providing all the research facilities for this work.

Authors' contributions

Doaa Khodary Zater: Investigation, methodology, formal analysis, data curation, and writing of the original draft. Fatma I. Elzamik: funding acquisition, review and editing of the manuscript. Howaida M. Abdel basit: formal analysis, data curation, visualization, review and editing of the manuscript. G. M. Moustafa: formal analysis, data curation, visualization, review and editing of the manuscript. Dena Z. Khater: conceptualization, investigation, methodology, formal analysis, data curation, visualization, validation, writing, review and editing of the manuscript. Kamel M. El-Khatib: conceptualization, data curation, visualization, validation, review and editing of the manuscript and supervision. All the authors have read and agreed to the published version of the manuscript.

Funding

Open access funding provided by The Science, Technology & Innovation Funding Authority (STDF) in cooperation with The Egyptian Knowledge Bank (EKB). This work was financially supported by Zagazig University and the National Research Centre. The study was supported for publication by open access funding provided by the Science, Technology & Innovation Funding Authority (STDF) in cooperation with the Egyptian Knowledge Bank (EKB).

Availability of data and materials

All the data generated or analysed during this study are included in this article.

Declarations

Ethics approval and consent to participate

This article does not contain any studies with human participants or animals performed by any of the authors.

Competing interests

The authors declare that they have no competing interests.

Received: 26 January 2024 Accepted: 2 May 2024

Published online: 27 May 2024

References

- Rahman TU, Roy H, Islam MR, Tahmid M, Fariha A, Mazumder A, et al. The advancement in membrane bioreactor (MBR) technology toward sustainable industrial wastewater management. *Membranes*. 2023;13:181.
- Samudro G, Imai T, Hung YT. Enhancement of power generation and organic removal in double anode chamber designed dual-chamber microbial fuel cell (DAC-DCMFC). *Water*. 2021;13:2941.
- Fadzli FS, Bhawani SA, Adam Mohammad RE. Microbial fuel cell: recent developments in organic substrate use and bacterial electrode interaction. *J Chem-Ny*. 2021;2021:4570388.
- Xiao L, Li J, Lichtfouse E, Li Z, Wang Q, Liu F. Augmentation of chloramphenicol degradation by *Geobacter*-based biocatalysis and electric field. *J Hazard Mater*. 2021;410:124977.
- Costa NL, Clarke TA, Philipp LA, Gescher J, Louro RO, Paquete CM. Electron transfer process in microbial electrochemical technologies: The role of cell-surface exposed conductive proteins. *Bioresource Technol*. 2018;255:308–17.
- Yang Y, Xu M, Guo J, Sun G. Bacterial extracellular electron transfer in bioelectrochemical systems. *Process Biochem*. 2012;47:1707–14.
- Martinez CM, Alvarez LH. Application of redox mediators in bioelectrochemical systems. *Biotechnol Adv*. 2018;36:1412–23.
- Bose D, Bhattacharya R, Mukherjee A. Bibliometric analysis of research trends in microbial fuel cells for wastewater treatment. *Biochem Eng J*. 2024;202:109155.
- Reguera G, McCarthy KD, Mehta T, Nicoll JS, Tuominen MT, Lovley DR. Extracellular electron transfer via microbial nanowires. *Nature*. 2005;435:1098–101.
- Zhi W, Ge Z, He Z, Zhang H. Methods for understanding microbial community structures and functions in microbial fuel cells: A review. *Bioresource Technol*. 2014;171:461–8.
- Peera SG, Maiyalagan T, Liu C, Ashmath S, Lee TG, Jiang Z, et al. A review on carbon and non-precious metal based cathode catalysts in microbial fuel cells. *Int J Hydrogen Energ*. 2021;46:3056–89.
- Khater DZ, Amin RS, Fetohi AE, Mahmoud M, El-Khatib KM. Insights on hexavalent chromium(VI) remediation strategies in abiotic and biotic dual chamber microbial fuel cells: electrochemical, physical, and metagenomics characterizations. *Sci Rep-Uk*. 2023;13:20184.
- Kim HJ, Park HS, Hyun MS, Chang IS, Kim M, Kim BH. A mediator-less microbial fuel cell using a metal reducing bacterium, *Shewanella putrefaciens*. *Enzyme Microb Tech*. 2002;30:145–52.
- Min B, Cheng S, Logan BE. Electricity generation using membrane and salt bridge microbial fuel cells. *Water Res*. 2005;39:1675–86.
- Bond DR, Lovley DR. Electricity Production by *Geobacter sulfurreducens* Attached to Electrodes. *Appl Environ Microb*. 2003;69:1548–55.
- Chaudhuri SK, Lovley DR. Electricity generation by direct oxidation of glucose in mediatorless microbial fuel cells. *Nat Biotechnol*. 2003;21:1229–32.
- Al-Ansari MM, Benabdelkamel H, Al-Humaid L. Degradation of sulfadiazine and electricity generation from wastewater using *Bacillus subtilis* EL06 integrated with an open circuit system. *Chemosphere*. 2021;276:130145.
- Pandey P, Shinde VN, Deopurkar RL, Kale SP, Patil SA, Pant D. Recent advances in the use of different substrates in microbial fuel cells toward wastewater treatment and simultaneous energy recovery. *Appl Energ*. 2016;168:706–23.
- Zhao Q, Yu H, Zhang W, Kabutey FT, Jiang J, Zhang Y, et al. Microbial fuel cell with high content solid wastes as substrates: a review. *Front Env Sci Eng*. 2017;11:13.
- Bai X, Lin T, Liang N, Li BZ, Song H, Yuan YJ. Engineering synthetic microbial consortium for efficient conversion of lactate from glucose and xylose to generate electricity. *Biochem Eng J*. 2021;172:108052.
- Kaur R, Marwaha A, Chhabra VA, Kim KH, Tripathi SK. Recent developments on functional nanomaterial-based electrodes for microbial fuel cells. *Renew Sustain Energy Rev*. 2020;119:109551.
- Khodary D, Elzamik F, Abdelbasit HML, Moustafa GM, El Khatib KM. Wastewater treatment and electricity generation via microbial fuel cell using ZnO supported on activated carbon cathode electrocatalyst. *Egypt J Chem*. 2023;66:1015–24.
- Pinto RP, Srinivasan B, Guiot SR, Tartakovsky B. The effect of real-time external resistance optimization on microbial fuel cell performance. *Water Res*. 2011;45:1571–8.
- Fernando E, Keshavarz T, Kyazze G. External resistance as a potential tool for influencing azo dye reductive decolourisation kinetics in microbial fuel cells. *Int Biodeter Biodegr*. 2014;89:7–14.
- Hu X, Liu J, Cheng W, Li X, Zhao Y, Wang F, et al. Synergistic interactions of microbial fuel cell and microbially induced carbonate precipitation technology with molasses as the substrate. *Environ Res*. 2023;228:115849.
- Feng Y, Wang X, Logan BE, Lee H. Brewery wastewater treatment using air-cathode microbial fuel cells. *Appl Microbiol Biot*. 2008;78:873–80.
- Sharma M, Sarma PM, Pant D, Dominguez-Benetton X. Optimization of electrochemical parameters for sulfate-reducing bacteria (SRB) based biocathode. *RSC Adv*. 2015;5:39601–11.

28. Eigner U, Schmid A, Wild U, Bertsch D, Fahr AM. Analysis of the comparative workflow and performance characteristics of the VITEK 2 and Phoenix systems. *J Clin Microbiol.* 2005;43:3829–34.
29. Khater DZ, Amin RS, Zhran MO, Abd El-Aziz ZK, Mahmoud M, Hassan HM, et al. The enhancement of microbial fuel cell performance by anodic bacterial community adaptation and cathodic mixed nickel–copper oxides on a graphene electrocatalyst. *J Genet Eng Biotechnol.* 2022;20:12.
30. Basson A, Flemming LA, Chenia HY. Evaluation of adherence, hydrophobicity, aggregation, and biofilm development of *Flavobacterium johnsoniae*-like isolates. *Microb Ecol.* 2008;55:1–14.
31. Yap KL, Ho LN, Ong SA, Guo K, Oon YS, Ong YP, et al. Crucial roles of aeration and catalyst on caffeine removal and bioelectricity generation in a double chambered microbial fuel cell integrated electrocatalytic process. *J Environ Chem Eng.* 2021;9:104636.
32. Mathew S, Thomas PC. Fabrication of polyaniline nanocomposites as electrode material for power generation in microbial fuel cells. *Mater Today-Proc.* 2020;33:1415–9.
33. Tajdid Khajeh R, Aber S, Nofouzi K. Efficient improvement of microbial fuel cell performance by the modification of graphite cathode via electrophoretic deposition of CuO/ZnO. *Mater Chem Phys.* 2020;240:122208.
34. Dessie Y, Tadesse S, Eswaramoorthy R. Surface roughness and electrochemical performance properties of biosynthesized α -MnO₂/NiO-based polyaniline ternary composites as efficient catalysts in microbial fuel cells. *J Nanomater.* 2021;2021:7475902.
35. Ghasemi M, Wan Daud WR, Hassan SHA, Jafary T, Rahimnejad M, Ahmad A, et al. Carbon nanotube/polypyrrole nanocomposite as a novel cathode catalyst and proper alternative for Pt in microbial fuel cell. *Int J Hydrogen Energ.* 2016;41:4872–8.
36. Ghasemi M, Sedighi M, Tan YH. Carbon nanotube/Pt cathode nanocomposite electrode in microbial fuel cells for wastewater treatment and bioenergy production. *Sustainability.* 2021;13:8057.
37. Din MI, Ahmed M, Ahmad M, Iqbal M, Ahmad Z, Hussain Z, et al. Investigating the activity of carbon fiber electrode for electricity generation from waste potatoes in a single-chambered microbial fuel cell. *J Chem-Ny.* 2023;2023:8520657.
38. Bahamonde Soria R, Chinchin BD, Arboleda D, Zhao Y, Bonilla P, Van der Bruggen B, et al. Effect of the bio-inspired modification of low-cost membranes with TiO₂/ZnO as microbial fuel cell membranes. *Chemosphere.* 2022;291:132840.
39. Prasad D, Arun S, Murugesan M, Padmanaban S, Satyanarayanan RS, Berchmans S, et al. Direct electron transfer with yeast cells and construction of a mediatorless microbial fuel cell. *Biosens Bioelectron.* 2007;22:2604–10.
40. Kato Marcus A, Torres CI, Rittmann BE. Conduction-based modeling of the biofilm anode of a microbial fuel cell. *Biotechnol Bioeng.* 2007;98:1171–82.
41. Venkidusamy K, Megharaj M. Identification of electrode respiring, hydrocarbonoclastic bacterial strain *Stenotrophomonas maltophilia* MK2 highlights the untapped potential for environmental bioremediation. *Front Microbiol.* 2016;7:1965.
42. Zanolli G, Di Toro S, Todaro D, Varese GC, Bertolotto A, Fava F. Characterization of two diesel fuel degrading microbial consortia enriched from a non acclimated, complex source of microorganisms. *Microb Cell Fact.* 2010;9:10.
43. Sotres A, Diaz-Marcos J, Guivernau M, Illa J, Magri A, Prenafeta-Boldu FX, et al. Microbial community dynamics in two-chambered microbial fuel cells: effect of different ion exchange membranes. *J Chem Technol Biotechnol.* 2015;90:1497–506.
44. Flimban S, Oh SE, Joo JH, Hussein KA. Characterization and identification of cellulose-degrading bacteria isolated from a microbial fuel cell reactor. *Biotechnol Bioproc E.* 2019;24:622–31.
45. Nachammai KT, Ramachandran S, Nagarajan C, Kulanthaivel L, Subbaraj GK, Chandrasekaran K, et al. Exploration of bioinformatics on microbial fuel cell technology: trends, challenges, and future prospects. *J Chem-Ny.* 2023;2023:6902054.
46. Khater DZ, Amin RS, Zhran MO, Abd El-Aziz ZK, Hassan HM, Mahmoud M, et al. Overcoming the bottlenecks of cellulose utilization in microbial fuel cells via bioaugmentation strategy with cellulose-degrading isolates. *Egypt J Chem.* 2023;66:371–80.
47. Bose D, Bhattacharya R, Gopinath M, Vijay P, Krishnakumar B. Bioelectricity production and bioremediation from sugarcane industry wastewater using microbial fuel cells with activated carbon cathodes. *Results Eng.* 2023;18:101052.
48. Silha D, Syrova P, Syrova L, Janeckova J. Smoothie drinks: possible source of resistant and biofilm-forming microorganisms. *Foods.* 2022;11:4039.
49. O'Toole G, Kaplan HB, Kolter R. Biofilm formation as microbial development. *Annu Rev Microbiol.* 2000;54:49–79.

Publisher's Note

Springer Nature remains neutral with regard to jurisdictional claims in published maps and institutional affiliations.